a process is probable in an organic solvent, where the chances of a static quenching of the ^3MC by Cl^- within an ion pair are increased. In agreement with this is the fact that, in water, we have not observed any quenching of $Ru(tap)_3^{2+*}$ by Cl^- even with concentrations as high as 1 M.

The mechanism proposed above has already been mentioned previously in the literature,[49] without however giving experimental evidence in its favor. In our case, the results are in agreement with the proposed equilibrium; however no definite proof has been established up to now.

3. Combined Temperature and Cl^- Effects. The comparison of the lifetime dependence of $Ru(tap)_3^{2+*}$ on temperature, in the absence and in the presence of Cl^-, provides much more information on the system and allows us to draw more definite conclusions.

The parameters of eq i derived from these experiments are also given in Table IV; we shall examine the effect of Cl^- on each of them.

The sum of $k_r + k_{nr}$ is not affected by Cl^-, within the experimental errors; consequently, the observed luminescence quenching by Cl^- does not stem from a quenching of the ^3MLCT, for example by electron transfer, as one could think a priori. In contrast, the values of k' and ϕ_{dd} are increased by Cl^-, showing thus that Cl^- plays some role in the crossing-over to the ^3MC; if we compare the $\Delta E'$ values, it does not seem that Cl^- has an effect on the energy barrier, which remains constant, taking into account the experimental error on $\Delta E'$. As shown by comparing the preexponential factors values, it is clear that Cl^- increases k^∞ by a factor of 3. In the case of an irreversible process, k^∞ should be equal to the preexponential factor of the rate constant k_2, corresponding to the crossing to the ^3MC; an effect of Cl^- on this factor would be difficult to explain. On the contrary, in the case of an equilibrium,[32,49-51] k^∞ would then be equal to k_3, the global constant containing the different factors contributing to the decay of ^3MC; in that case, it becomes easier to explain the enhancement of the ^3MC decay by Cl^-. The reaction of Cl^- with ^3MC would be so rapid (static quenching) that it would shift the equilibrium toward the reacting ^3MC, leading to photoproducts. At this stage, it is useless to try to correlate some rate constant of reaction deriving from k^∞ (k_3) with the approximate quenching rate constant that we found for the luminescence quenching by Cl^- (2×10^{10} M^{-1} s^{-1}); indeed, if the photophysical mechanism that we propose is correct, τ_0/τ versus the concentration of Cl^- does not correspond to a simple Stern-Volmer plot but to a more complicated function that we cannot test experimentally for the reasons mentioned before.

If we return to the comparison between $Ru(tap)_3^{2+}$ and $Ru(bpz)_3^{2+}$, we may conclude the following. Taking into account the published data on $Ru(bpz)_3^{2+}$ [49b] and our data on $Ru(tap)_3^{2+}$, it seems that the photophysics of $Ru(bpz)_3^{2+}$ would be intermediate between that of $Ru(tap)_3^{2+}$ and that of $Ru(bpy)_3^{2+}$. As mentioned previously, the flash-photolysis results[1b] indicate some similarities between $Ru(bpz)_3^{2+}$ and $Ru(tap)_3^{2+}$. However one cannot conclude that the photophysical mechanism is the same (equilibrium between ^3MLCT and ^3MC) because the lifetime dependence on temperature has not been measured for $Ru(bpz)_3^{2+}$. The two striking differences between the photochemistries of $Ru(bpz)_3^{2+}$ and $Ru(tap)_3^{2+}$ (lower ϕ_D and intermediate photodechelation product) could easily be explained: after the first photochemical breaking of the N-Ru bond from the ^3MC states of the complexes, the nitrogen of the rigid and planar tap ligand would coordinate back to the metal more easily than the nitrogen of the more flexible bpz ligand.

Conclusion

The study presented here points out the interesting photophysical behavior of $Ru(tap)_3^{2+}$ in its ^3MLCT excited state. The results suggest, more especially the dependence of the luminescence lifetime on temperature, in absence and presence of Cl^-, that the ^3MLCT state is dynamically coupled to the ^3MC through a rapid equilibrium, at least in acetonitrile. On the other hand, the two other members of the series of tap complexes $Ru(bpy)_n(tap)_{3-n}^{2+}$ (n = 1, 2) present properties similar to those already described for other series of heteroleptic complexes (with bpy and bipyrazine for instance[49]), as is evidenced from their "classical" dependence of luminescence lifetime on solvent and temperature (room temperature versus 77 K). This peculiar behavior of $Ru(tap)_3^{2+}$ makes it very sensitive to its close environment, so that this complex is an ideal probe to test different microenvironments of different polymers such as the ion exchanger Sephadex SP-C25 or Nafion membranes, which are currently under investigation.

Acknowledgment. L.J. wishes to thank the Institut pour l'Encouragement de la Recherche Scientifique dans l'Industrie et l'Agriculture (IRSIA) for a fellowship.

Contribution from the Institut für Theoretische Chemie, Universität Stuttgart, Pfaffenwaldring 55, 7000 Stuttgart 80, Federal Republic of Germany, and Max-Planck-Institut für Festkörperforschung, Heisenbergstrasse 1, 7000 Stuttgart 80, Federal Republic of Germany

Pseudopotential Investigations on the Molecules Cu_2Si_2, Cu_2Sn_2, Cu_4Si_4, and Cu_4Sn_4

W. Plass,*,† A. Savin,† H. Stoll,† H. Preuss,† R. Nesper,‡ and H.-G. von Schnering‡

Received January 9, 1989

Pseudopotential calculations have been performed to obtain the binding energy and the equilibrium geometry of the clusters Cu_2X_2 and Cu_4X_4 with X = Si and Sn. Several possible structures have been taken into account. The equilibrium structures are the butterfly arrangement for the Cu_2X_2 clusters and the heterocubane arrangement for the Cu_4X_4 clusters. For the latter ones a new competitive structure with copper atoms in μ_2-bridging positions is found. The bonding situation has been analyzed by means of population analysis, internally consistent self-consistent-field energies, and localized orbitals. For simulating the lower valence of the X atoms, we have performed molecular calculations where the corresponding valence s orbitals are kept frozen. The "inert pair effect" and multicenter contributions to chemical bonding are discussed.

Introduction

In the last three decades the interest on mixed clusters of group 11 and group 14 elements has been increasing due to their importance in areas like catalysis, crystal growth, semiconductors, and intermetallic phases.[1-5] Up to now the bulk of experimental data of these mixed clusters exists for the clusters containing the heavier elements of both groups;[6-10] however, neither experimental nor theoretical work about their structure has been published. For

† Universität Stuttgart.
‡ Max-Planck-Institut für Festkörperforschung.

(1) Sinfelt, J. H. *J. Catal.* **1973**, *29*, 308; *Acc. Chem. Res.* **1977**, *10*, 15.
(2) Yacaman, M. J.; Dominguez, J. M. *J. Catal.* **1981**, *67*, 475.
(3) Abraham, F. F. *Homogeneous Nucleation Theory*; Academic Press: New York, 1974.
(4) Baetzold, R. C.; Mack, R. E. *J. Chem. Phys.* **1975**, *62*, 1513.
(5) Gates, B. C.; Lieto, J. *Chem. Technol.* **1980**, *10*, 195, 248.
(6) Gingerich, K. A.; Hague, R.; Kingcade, J. E. *Thermochim. Acta* **1978**, *30*, 61.

0020-1669/90/1329-0860$02.50/0

the corresponding clusters of group 1 and group 14 elements solid-state structures[11-14] as well as molecular beam experiments are known[15] (for a review see ref 16). Also, results of quantum chemical calculations (pseudopotential as well as all-electron) have been published for Li_2C_2, Li_4C_4,[17-20] Li_2Si_4,[21] Li_2Si_2, Na_2Si_2, Li_4Si_4, and Na_4Si_4.[22] Similar calculations have been done for the hydrogen compounds of silicon (Si_2H_2[23-27] and Si_4H_4[28,29]). In comparison to clusters composed of group 1 and group 14 elements, the question still holds whether mixed clusters containing group 11 elements will show similar structures and properties, especially, whether an anionic X_2 and X_4 backbone exists, which is characteristic for molecules that belong to the so-called Zintl compounds.[30-33] Therefore, a corresponding theoretical investigation on mixed clusters of group 11 and group 14 elements seems to be worthwhile.

In the present paper we concentrated on Cu_2X_2 and Cu_4X_4 clusters (X = Si, Sn) and investigated the relative stability of several possible arrangements (cf. Figures 1 and 2; structures **4–7** have only been treated for X = Sn). For the corresponding Au_2Ge_2 clusters Kingcade et al. have been assumed that a linear structure is the most stable one related to their experimental thermodynamic data.[9] Moreover, effects of valence correlation are discussed for the optimized cluster topology. The results are analyzed by means of population analysis,[34] internally consistent self-consistent-field (ICSCF) energies,[35] and localized molecular orbitals (LMO).[36] Furthermore, we have performed molecular calculations where the s orbitals of the X atoms are kept frozen, according to the expectation that only the p orbitals of the X atoms must be treated as valence shell, what is often called the "inert pair effect" (e.g., see ref 37).

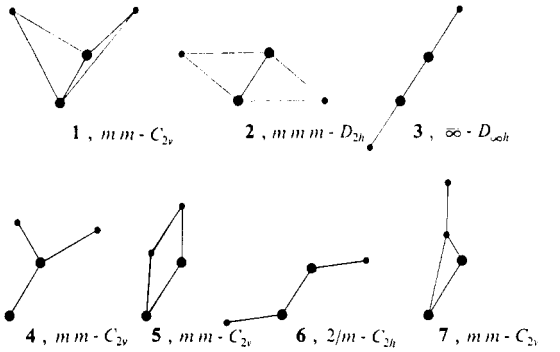

Figure 1. Structures and point symmetry groups of hypothetical Cu_2X_2 clusters **1–7** (**4–7** only for Cu_2Sn_2): X, large circles; Cu, small circles.

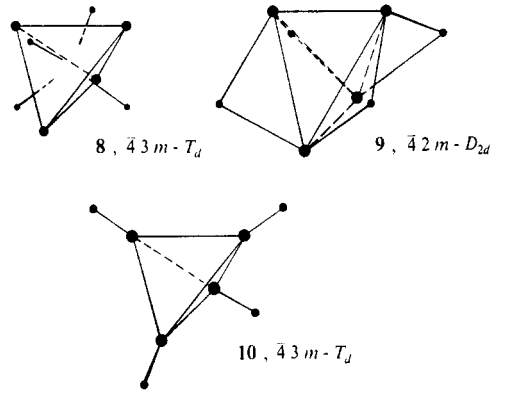

Figure 2. Structures and point symmetry groups of the Cu_4X_4 clusters investigated (**8–10**): X, large circles; Cu, small circles.

Method

In order to reduce the computational effort and to treat all elements within a column of the periodic table on equal footing, we applied the pseudopotential method.[38,39] Copper is treated as a one-valence-electron atom (for the validity of this approach, see e.g. refs 40–43), and silicon and tin are treated as four-valence-electron atoms,[44,45] respectively. The pseudopotential method has the additional advantage that relativistic effects can be included in a simple way.[46-48] The valence model Hamiltonian (in atomic units) used in our calculations is

$$H_{mod} = -\frac{1}{2}\sum_i \Delta_i + \sum_i \sum_\lambda V_\lambda(r_{\lambda i}) + \sum_{i<j} \frac{1}{r_{ij}} + \sum_{\lambda<\mu} \frac{Q_\lambda Q_\mu}{r_{\lambda\mu}} \qquad (1)$$

(i and j denote valence electrons, λ and μ are core indices). Q_λ is the charge of the core λ. $V_\lambda(r_{\lambda i})$ is a semilocal pseudopotential of the form

$$V_\lambda(r_{\lambda i}) = -\frac{Q_\lambda}{r_{\lambda i}} + \sum_l \sum_k B_{lk}^\lambda \exp(-\beta_{lk}^\lambda r_{\lambda i}^2) P_l^\lambda \qquad (2)$$

P_l^λ is the projection operator on angular momentum l with respect to core λ. The parameters B_{lk}^λ and β_{lk}^λ have been adjusted to experimental and Dirac–Fock (DF) ionization and excitation energies of the one-valence-electron ions. The pseudopotential parameters used in this work have

(7) Kingcade, J. E.; Gingerich, K. A. *J. Chem. Phys.* **1986**, *84*, 3432.
(8) Kingcade, J. E.; Gingerich, K. A.; Choudary, U. V. *J. Phys. Chem.* **1978**, *82*, 49.
(9) Kingcade, J. E.; Choudary, U. V.; Gingerich, K. A. *Inorg. Chem.* **1979**, *18*, 3094.
(10) Kingcade, J. E.; Dufner, D. C.; Gupta, S. K.; Gingerich, K. A. *High Temp. Sci.* **1978**, *10*, 213.
(11) von Schnering, H. G.; Nesper, R.; Tebbe, K. F.; Curda, J. *Z. Metallkd.* **1980**, *71*, 357.
(12) Bussmann, E. *Z. Anorg. Allg. Chem.* **1961**, *313*, 90.
(13) Witte, J.; von Schnering, H. G. *Z. Anorg. Allg. Chem.* **1964**, *327*, 260.
(14) Llanos, J. Thesis, University of Stuttgart, West Germany, 1984.
(15) Martin, T. P. *J. Chem. Phys.* **1985**, *83*, 78.
(16) Martin, T. P. *Angew. Chem., Int. Ed. Engl.* **1986**, *25*, 197.
(17) Rauscher, G.; Clark, T.; Poppinger, D.; Schleyer, P. v. R. *Angew. Chem., Int. Ed. Engl.* **1978**, *17*, 276.
(18) Schleyer, P. v. R. *Pure Appl. Chem.* **1984**, *50*, 151.
(19) Ritchie, J. P. *J. Am. Chem. Soc.* **1983**, *105*, 1983.
(20) Disch, R. L.; Schulman, J. M.; Ritchie, J. P. *J. Am. Chem. Soc.* **1984**, *106*, 6246.
(21) Krough-Jespersen, K. *J. Am. Chem. Soc.* **1985**, *107*, 537.
(22) Savin, A.; Vogel, K.; Preuss, H.; Stoll, H.; Nesper, R.; von Schnering, H. G. *J. Am. Chem. Soc.* **1988**, *110*, 373.
(23) Lischka, H.; Köhler, H. J. *J. Am. Chem. Soc.* **1983**, *105*, 6646.
(24) Köhler, H. J.; Lischka, H. *Chem. Phys. Lett.* **1984**, *112*, 33.
(25) Binkley, J. S. *J. Am. Chem. Soc.* **1984**, *106*, 603.
(26) Kalcher, J.; Sax, A.; Olbrich, G. *Int. J. Quantum Chem.* **1984**, *25*, 5341.
(27) Luke, B. T.; Pople, J. A.; Krough-Jespersen, M. B.; Apeloig, Y.; Karni, M.; Chandrasekhar, J.; Schleyer, P. von Ragué *J. Am. Chem. Soc.* **1986**, *108*, 270.
(28) Clabo, D. A.; Schaefer, H. F., III *J. Am. Chem. Soc.* **1986**, *108*, 4344.
(29) Yates, B. F.; Clabo, D. A.; Schaefer, H. F., III. *Chem. Phys. Lett.* **1988**, *143*, 421.
(30) Zintl, E. *Angew. Chem.* **1939**, *52*, 1. Laves, F. *Naturwissenschaften* **1941**, *29*, 244.
(31) von Schnering, H. G. *Angew. Chem., Int. Ed. Engl.* **1981**, *20*, 33.
(32) Corbett, J. D. *Chem. Rev.* **1985**, *85*, 383.
(33) Schäfer, H. *Annu. Rev. Mater. Sci.* **1985**, *15*, 1.
(34) Davidson, E. R. *J. Chem. Phys.* **1967**, *46*, 3320.
(35) Zeller-Stenkamp, L.; Davidson, E. R. *Theor. Chim. Acta* **1973**, *30*, 283.
(36) Foster, S.; Boys, S. F. *Rev. Mod. Phys.* **1960**, *32*, 296.
(37) Sidgwick, N. V. *The Covalent Link in Chemistry*; Cornell University Press: Ithaca, NY, 1933.
(38) Weeks, J. D.; Hazi, A.; Rice, S. A. *Adv. Chem. Phys.* **1969**, *16*, 283.
(39) Krauss, M.; Stevens, W. J. *Annu. Rev. Phys. Chem.* **1984**, *35*, 357.
(40) Stoll, H.; Fuentealba, P.; Dolg, M.; Flad, J.; von Szentpály, L.; Preuss, H. *J. Chem. Phys.* **1983**, *79*, 5532.
(41) Stoll, H.; Fuentealba, P.; Schwerdtfeger, P.; Flad, J.; von Szentpály, L.; Preuss, H. *J. Chem. Phys.* **1984**, *81*, 2732.
(42) Igel, G.; Wedig, U.; Dolg, M.; Fuentealba, P.; Preuss, H.; Stoll, H. *J. Chem. Phys.* **1984**, *81*, 2737.
(43) Plass, W.; Savin, A.; Preuss, H.; Stoll, H. To be submitted for publication.
(44) Igel-Mann, G.; Stoll, H.; Preuss, H. *Mol. Phys.* **1988**, *65*, 1321.
(45) Igel-Mann, G.; Stoll, H.; Preuss, H. *Mol. Phys.* **1988**, *65*, 1329.
(46) Kutzelnigg, W. *Phys. Scr.* **1987**, *36*, 416.
(47) Schwerdtfeger, P. *Phys. Scr.* **1987**, *36*, 453.
(48) Pyykkö, P. *Chem. Rev.* **1988**, *88*, 563.

Table I. SCF Geometry, Harmonic Frequencies, and Valence Energies for Cu_2Sn_2 Conformers

conformer	symmetry	geometry[a]		valence energy[b,e]		harmonic freq[c]	
1	*mm*-C_{2v}	R_{Sn-Sn}	2.68	SCF + Δ	−7.1124	A_1	47
		R_{Cu-Sn}	2.76	+SPP	−7.3169		140
		∠(Cu−M−Cu)[d]	81.5	+GCP	−7.4046		210
						A_2	81
						B_1	143
						B_2	90
2	*mmm*-D_{2h}	R_{Sn-Sn}	2.72	SCF + Δ	−7.0818	A_g	153
		R_{Cu-Sn}	2.68	+SPP	−7.2855		235
				+GCP	−7.3736	B_{1g}	80
						B_{1u}	63 (i)
						B_{2u}	192
						B_{3u}	78
3	∞-$D_{\infty h}$	R_{Sn-Sn}	2.45	SCF + Δ	−7.0385	Σ_g^+	153
		R_{Cu-Sn}	2.52	+SPP	−7.2417		313
				+GCP	−7.3262	Σ_u^+	248
						Π_g	39 (i)
						Π_u	30
4	*mm*-C_{2v}	R_{Sn-Sn}	2.63	SCF + Δ	−7.0736	A_1	35
		R_{Cu-Sn}	2.55	+SPP	−7.2769		151
		∠(Cu−Sn−Cu)	130.0	+GCP	−7.3588		241
						B_2	20
5	*mm*-C_{2v}	R_{Sn-Sn}	2.63	SCF + Δ	−7.0525	A_1	143
		R_{Cu-Sn}	2.65	+SPP	−7.2558		166
		R_{Cu-Cu}	2.55	+GCP	−7.3406		238
						A_2	98 (i)
6	2/*m*-C_{2h}	R_{Sn-Sn}	2.55	SCF + Δ	−7.0581	A_g	71
		R_{Cu-Sn}	2.56	+SPP	−7.2613		232
		∠(Sn−Sn−Cu)	126.6	+GCP	−7.3441		286
						A_u	41 (i)
7	*mm*-C_{2v}	R_{Sn-Sn}	2.75	SCF + Δ	−7.0226	A_1	79
		R_{Cu-Sn}	2.75	+SPP	−7.2214		182
		R_{Cu-Cu}	2.44	+GCP	−7.2983		191
						B_2	114 (i)

[a] Bond distances are in angstroms, and bond angles, in degrees. [b] Valence energies are in atomic units (1 au = 1 hartree = 2.626 MJ/mol), at SCF level including core–core interaction (SCF + Δ); plus valence correlation energy according to the density functional of Stoll, Pavlidou, and Preuss (+SPP) and according to that suggested by Perdew (+GCP). [c] Harmonic frequencies are in cm^{-1}; imaginary frequencies are denoted by i. [d] M is the midpoint of the X–X bond. [e] $E_{SCF}(Cu, {}^1S) = -0.2446$ au. $E_{SCF}(Sn, {}^3P) = -3.2493$ au. $E_{SCF}(Sn_2, {}^3\Sigma_g^-, R = 2.71$ Å, equilibrium bond length) = −6.5378 au.

been taken from ref 40 (Cu) and ref 44 (Si, Sn), respectively.

Valence self-consistent-field (SCF) calculations have been done with the program MELD[49] using small basis sets, which had been energy optimized[50] for the ground states of the neutral atoms. For the highest *l* value of the valence shell of each atom (p for Si and Sn; s for Cu) the basis sets were augmented by a diffuse function optimized for the corresponding anion to ensure a reliable description for both possible anionic species X^- and Cu^-. This, of course, is important, since it is not known whether X^- anions (like Zintl phases) will occur or not (X = Si, Sn). By adding polarization functions,[51] we obtained a [31/211/1] Gaussian type orbital (GTO) basis set for silicon and tin and a [211/11] GTO basis set for copper[43] (for notation, see ref 52).

It became apparent in calculations of dimers and hydrides containing copper[40] that in the case of a one-electron pseudopotential the core–core interaction could not be treated within a simple point charge model. Deviations from the point charge interactions have been derived from frozen-core SCF pseudopotential interaction curves of $Cu^+\cdots X^{4+}$ and have been fitted to an exponential function of the form $\Delta = D\exp(-\eta R)$ (for parameters, see ref 43). We applied a 19-electron pseudopotential for copper and a 22-electron pseudopotential for tin (pseudopotential parameters and GTO basis sets given in ref 43) and took all electrons into account for silicon.

Valence correlation effects have been investigated for the most stable geometry within the chosen symmetry by use of density functional methods.[53,54] In this work two different density functionals were used, one with the self-interaction correction of Stoll, Pavlidou, and Preuss (SPP)[55] and the other with a gradient correction suggested by Perdew (GCP)[56] (for parametrization, see ref 54 and references therein). To check the density functional results, configuration interaction (CI) calculations with all single and double excitations from the SCF reference configuration (CI–SD) have been performed. In the case of Cu_2Sn_2 additional CI–SD calculations with an augmented [311/2111/11] GTO basis set for tin have been done.

The results for the treatment of copper as a one-valence-electron atom are verified in the case of Cu_2Si_2 and Cu_2Sn_2 by comparison with a full CI–SD calculation with a 11-electron pseudopotential and the corresponding [111/11/311] GTO basis set for copper.[57]

Vibrational frequencies have been calculated for the optimized structures by fitting harmonic potentials for symmetry-adapted internal coordinates[58,59] in order to get information about the rigidity of molecules and their possible distortions. (For optimization the internal coordinates belonging to the total symmetric irreducible representation are used in the harmonic potential.)

Furthermore, to investigate the nature of the bonding and lone pairs, an orbital picture has been applied: ICSCF orbitals[35] as well as LMOs[36] were determined. We also used the population analysis of Davidson et al.[34] further developed by Roby[60] and Ahlrichs et al.,[61,62] which yields

(49) McMulchie, L.; Elbert, S.; Langhoff, S.; Davidson, E. R. "Program MELD"; University of Washington: Seattle, WA.
(50) Barthelat, J. C.; Durand, P. "Program PSATOM"; Université Paul Sabatier: Toulouse, France. This is a modified version of the program ATOM-JCF written by: Roos, B.; Salez, C.; Veillard, A.; Clementi, E. Technical Report RJ 518; IBM Research: Armonk, NY, 1968.
(51) For silicon and tin the polarization functions were optimized to yield a maximum in the binding energy of the dimers X_2. For copper, we took the two lowest *p* exponents from a (8s,7p,6d)-GTO basis set, optimized for a 19-valence electron pseudopotential (cf. ref 43).
(52) Huzinaga, S.; Andzelm, J.; Klobukowski, M.; Radzio-Andzelm, E.; Sakai, Y.; Tatewaki, H. *Gaussian Basis Sets for Molecular Calculations*; Elsevier: Amsterdam, 1984; p 3.
(53) Stoll, H.; Savin, A. In *Density Functional Methods in Physics*; Plenum Press: New York, 1985; p 177.
(54) Savin, A.; Stoll, H.; Preuss, H. *Theor. Chim. Acta* **1986**, *70*, 407.
(55) Stoll, H.; Pavlidou, C. M. E.; Preuss, H. *Theor. Chim. Acta* **1978**, *49*, 143.
(56) Perdew, J. P. *Phys. Rev.* **1986**, *B33*, 8822.
(57) Hay, P. J.; Wadt, W. R. *J. Chem. Phys.* **1985**, *82*, 270.
(58) Wilson, E. B.; Decius, J. C.; Cross, P. C. *Molecular Vibrations*; McGraw-Hill Book Co.: New York, 1955.
(59) Ferraro, J. R.; Ziomek, J. S. *Introductory Group Theory*; Plenum Press: New York, 1969.
(60) Roby, K. R. *Mol. Phys.* **1974**, *27*, 81.
(61) Heinzmann, R.; Ahlrichs, R. *Theor. Chim. Acta* **1976**, *42*, 33.

Table II. SCF Geometry, Harmonic Frequencies, and Valence Energies for Cu_2Si_2 Conformers

conformer	symmetry	geometry[a]		valence energy[b,e]		harmonic freq[c]	
1	mm-C_{2v}	R_{Si-Si}	2.16	SCF + Δ	−8.0456	A_1	57
		R_{Cu-Si}	2.49	+SPP	−8.2635		240
		∠(Cu–M–Cu)[d]	86.6	+GCP	−8.3571		595
						A_2	158
						B_1	231
						B_2	183
2	mmm-D_{2h}	R_{Si-Si}	2.15	SCF + Δ	−8.0220	A_g	183
		R_{Cu-Si}	2.43	+SPP	−8.2403		610
				+GCP	−8.3348		
3	∞-$D_{\infty h}$	R_{Si-Si}	2.02	SCF + Δ	−7.9914	Σ_g^+	188
		R_{Cu-Si}	2.30	+SPP	−8.2121		789
				+GCP	−8.3054		

[a] Bond distances are in angstroms, and bond angles, in degrees. [b] Valence energies are in atomic units (1 au = 1 hartree = 2.626 MJ/mol), at SCF level including core–core interaction (SCF + Δ); plus valence correlation energy according to the density functional of Stoll, Pavlidou, and Preuss (+SPP) and according to that suggested by Perdew (+GCP). [c] Harmonic frequencies are in cm^{-1}. [d] M is the midpoint of the X–X bond. $E_{SCF}(Si, {}^3P)$ = −3.6889 au. $E_{SCF}(Si_2, {}^3\Sigma_g^-, R = 2.21$ Å, equilibrium bond length) = −7.4450 au.

Table III. Relative Energy for Cu_2Sn_2 Conformers Relative to Structure **1** (mhartree)[a]

conformer	electronic state	SCF + Δ	SPP	GCP
1	$^1A_1$	0.0	0.0	0.0
2	$^1A_{1g}$	30.6	31.4	31.0
4	$^1A_1$	38.8	39.9	45.8
6	^1A_g	54.2	55.6	60.5
5	$^1A_1$	59.9	61.1	64.0
3	$^1\Sigma_g^+$	73.8	75.2	78.4
7	$^1A_1$	89.8	95.5	106.3

[a] 1 mhartree = 2.626 kJ/mol.

Table IV. Relative Energy for Cu_2Si_2 Conformers Relative to Structure **1** (mhartree)[a]

conformer	electronic state	SCF + Δ	SPP	GCP
1	$^1A_1$	0.0	0.0	0.0
2	$^1A_{1g}$	23.6	23.2	22.3
3	$^1\Sigma_g^+$	54.2	51.4	51.7

[a] 1 mhartree = 2.626 kJ/mol.

multicenter contributions to the chemical bond. This analysis is performed by a projection of the molecular electron density on a minimal atomic orbital (AO) basis set taken from atomic calculations. This leads to a multicenter expansion of the total molecular charge by means of shared electron numbers.

To investigate whether the s orbitals are involved in bond formation or not, frozen-core calculations with structural reoptimization have been performed. In these calculations for the Cu_2X_2 clusters, the two lowest molecular orbitals (MOs) were kept frozen and have only contributions of the s symmetry basis functions of the X atoms (Si and Sn). The coefficients were taken from atomic calculations for the ^3P ground states of silicon and tin.

Results and Discussion

For the mixed clusters of the type Cu_2X_2 and Cu_4X_4 (X = Si, Sn), we investigated the structures given in Figures 1 and 2. The corresponding data are summarized in Tables I, II, and V.

In the case of the Cu_2X_2 clusters we considered three principal arrangements (cf. Figure 1): a bent doubly bridged one (**1**), a planar doubly bridged one (**2**), and a linear one (**3**). To have a more detailed look at the potential energy surface, we additionally examined, in the case of Cu_2Sn_2, four possible structures belonging to the point groups mm-C_{2v} and $2/m$-C_{2h} (**4**–**7** in Figure 1).

For the Cu_2X_2 clusters we found structure **1** to be the most stable one similar to results from pseudopotential calculations on M_2Si_2 clusters with M ∈ group 1.[22] The relative thermodynamic stability (Tables III and IV) of structure **1** compared with **2**–**7** is rather high (the energy difference between the two most stable structures **1** and **2** is 58 kJ/mol for Cu_2Si_2 and 81 kJ/mol for Cu_2Sn_2), but the harmonic frequencies (Tables I and II) of these mixed clusters indicate a quite flat potential energy surface in the minimum region. The energetic separation between structures **1** and **2** in the case of the corresponding alkali-metal clusters M_2Si_2 is much lower (e.g. M = Li, 11 kJ/mol; M = Na, 13 kJ/mol) due to the greater ionic character of the chemical bonding. This can easily be rationalized by comparing the ionization potentials of copper and those of the alkali metals (Cu, 7.7 eV; Li, 5.4 eV; Cs, 3.9 eV).[62] Further indications are the charges in the corresponding M_2X_2 clusters, e.g. Cu_2Si_2 (Cu, ∼+0.4; Si, ∼−0.4) and Li_2Si_2 (Li, ∼+0.55; Si, ∼−0.55) (Table VII and ref 63).

Table V. Geometry[a] and Harmonic Frequencies[b] for Cu_2Si_2 with Structure **1** on Different Levels of Theory

	R_{Si-Si}	R_{Cu-Si}	∠(Cu–M–Cu)[c]	R_{Cu-Cu}	ω(A_1)		
			SCF				
1e PP for Cu	2.16	2.49	86.6	3.07	57	240	595
11e PP for Cu	2.17	2.57	88.2	3.23	57	205	592
			CI-SD				
11e PP for Cu	2.20	2.49	83.9	3.00	68	225	549

[a] Bond distances are in angstroms, and bond angles, in degrees. [b] Harmonic frequencies are in cm^{-1}. [c] M is the midpoint of the X–X bond.

The relative stability remains qualitatively unchanged when the basis set is enlarged and valence correlation effects are included by means of the local spin density (LSD) functional[54] or CI-SD calculations. For example, for the derived equilibrium structure of Cu_2Sn_2 we obtained with an extended basis set for tin quite the same energy difference between structures **1** and **2** (SCF 0.031 au; CI-SD 0.028 au) as with the smaller basis set (SCF 0.031 au; CI-SD 0.028 au). Inclusion of valence correlation effects only slightly changes the energetic separation between the structures **1**–**3** for the Cu_2X_2 molecules. Furthermore, the result is nearly independent whether density functional or CI-SD calculations have been performed (Cu_2Si_2: **2** − **1**, SPP 0.023 au, CI-SD 0.022 au; **3** − **1**, SPP 0.051 au, CI-SD 0.056 au. Cu_2Sn_2: **2** − **1**, SPP 0.031 au, CI-SD 0.028 au; **3** − **1**, SPP 0.075 au, CI-SD 0.073 au). Therefore, the density functional results seem to be a good qualitative approximation to include valence correlation effects in the case of the closed-shell molecules examined in this paper.

Correlation effects depending on excitations related with the d shell of copper are investigated by a CI-SD calculation with an 11-electron pseudopotential for the Cu_2X_2 molecules (structures **1**–**3**). The inclusion of the d shell yields no qualitative change of the energy differences on the CI-SD level for both molecules Cu_2Si_2 (**2** − **1**, 1 electron 0.022 au, 11 electrons 0.028 au; **3** − **1**, 1 electron 0.056 au, 11 electrons 0.054 au) and Cu_2Sn_2 (**2** − **1**, 1 electron 0.028 au, 11 electrons 0.034 au; **3** − **1**, 1 electron 0.073 au, 11 electrons 0.077 au). Also all geometry parameters of Cu_2Si_2 with structure **1** are nearly left unchanged if the geometry is reoptimized with the 11-electron pseudopotential for copper (see

(62) Erhardt, C.; Ahlrichs, R. *Theor. Chim. Acta* **1985**, *68*, 231.
(63) Moore, C. E. *Atomic Energy Levels*; National Bureau of Standards: Washington, DC, 1949.
(64) Vogel, K. Diplomarbeit, Institut für Theoretische Chemie, University of Stuttgart, West Germany, 1986.

Table VI. SCF Geometry and Valence Energies for Cu_4X_4 Conformers

conformer	symmetry	geometry[a]		valence energy[b,d]	
		Cu_4Si_4			
8	$\bar{4}3m$-T_d	R_{Si-Si}	2.51	SCF + Δ	−16.1615
		R_{Cu-Si}	2.48	+SPP	−16.6109
				+GCP	−16.8497
9	$\bar{4}2m$-D_{2d}	R_{Si-Si}	2.26	SCF + Δ	−16.1664
		R_{Si-Si}[c]	2.67	+SPP	−16.6138
		R_{Cu-Si}	2.43	+GCP	−16.8424
10	$\bar{4}3m$-T_d	R_{Si-Si}	2.34	SCF + Δ	−16.0698
		R_{Cu-Si}	2.31	+SPP	−16.5168
				+GCP	−16.7421
		Cu_4Sn_4			
8	$\bar{4}3m$-T_d	R_{Sn-Sn}	3.08	SCF + Δ	−14.2972
		R_{Cu-Sn}	2.74	+SPP	−14.7169
				+GCP	−14.9354
9	$\bar{4}2m$-D_{2d}	R_{Sn-Sn}	2.76	SCF + Δ	−14.2969
		R_{Sn-Sn}[c]	3.25	+SPP	−14.7156
		R_{Cu-Sn}	2.68	+GCP	−14.9250
10	$\bar{4}3m$-T_d	R_{Sn-Sn}	2.84	SCF + Δ	−14.1767
		R_{Cu-Sn}	2.53	+SPP	−14.5915
				+GCP	−14.7942

[a] Bond distances are in angstroms, and bond angles in degrees. [b] Valence energies are in atomic units (1 au = 1 hartree = 2.626 MJ/mol), at SCF level including core–core interaction (SCF + Δ); plus valence correlation energy according to the density functional of Stoll, Pavlidou, and Preuss (+SPP) and according to that suggested by Perdew (+GCP). [c] Length of the capped X_4 tetrahedrane edge. [d] $E_{SCF}(Si_4, T_d, R = 2.46$ Å, equilibrium bond length) = −14.9039 au. $E_{SCF}(Sn_4, T_d, R = 2.99$ Å, equilibrium bond length) = −13.0935 au.

Table VII. Relative Energy for Cu_4X_4 Conformers Relative to Structure **8** (mhartree)[a]

conformer	electronic state	SCF + Δ	SPP	GCP
		Cu_4Si_4		
8	$^1A_1$	0.0	0.0	0.0
9	$^1A_1$	−4.9	−2.9	7.3
10	^1A_g	94.7	94.1	107.6
2 × **1**	^1A_g	70.2	93.8	135.4
		Cu_4Sn_4		
8	$^1A_1$	0.0	0.0	0.0
9	$^1A_1$	0.3	1.3	10.4
10	^1A_g	120.5	125.4	141.2
2 × **1**	^1A_g	70.4	73.1	126.2

[a] 1 mhartree = 2.626 kJ/mol.

Table V). We will therefore use only the one-electron pseudopotential for copper.

For the dissociation of Cu_2X_2 clusters into two copper atoms and an X_2 unit, we found a binding energy of 230 kJ/mol (Si) and 190 kJ/mol (Sn) per copper atom, respectively, including valence correlation with the gradient corrected density functional of Perdew (GCP).[54,56] For the corresponding alkali-metal clusters the binding energy per metal atom is of the same order, e.g. 252 kJ/mol for Li_2Si_2 and 194 kJ/mol for Na_2Si_2,[22] respectively.

Cu_4X_4 clusters have been investigated for three different geometrical arrangements, all of them with a tetrahedral X_4 backbone (cf. Figure 2): copper atoms being in the μ_3-bridging position (heterocubane, **8**), copper atoms being in the μ_2-bridging position (tetrahedrane, with four capped edges, **9**), and copper atoms being terminally bonded (as in tetrahedrane, **10**). The corresponding calculated structures and the energies are summarized in Table VI.

A clear energetic separation, as for the Cu_2X_2 clusters, was not found for the Cu_4X_4 clusters (cf. Table VII). It is more difficult to decide whether structure **8** or **9** is the most stable one. For X = Si structure **9** is more stable than structure **8** by 13 kJ/mol, but in the case of X = Sn structure **8** is favored by 1 kJ/mol. With valence correlation effects included, structure **8** is found to be of lower energy in both cases (X = Si, Sn) by 19 and 27 kJ/mol, respectively. Additionally some test calculations were made on

Table VIII. Population Analysis Results for Cu_2X_2 Conformers **1–3**

	Cu_2Si_2			Cu_2Sn_2		
	1	**2**	**3**	**1**	**2**	**3**
			Atomic Occupations			
N_X	6.06	6.22	6.44	5.85	6.02	6.35
N_{Cu}	1.21	1.03	1.01	1.34	1.12	1.05
			Atomic Charges			
Q_X	−0.30	−0.42	−0.40	−0.22	−0.39	−0.38
Q_{Cu}	0.38	0.51	0.46	0.29	0.48	0.43
			Two Centers			
σ_{X-X}	2.64	2.76	3.13	2.32	2.35	2.96
σ_{Cu-X}	0.69	0.68	0.90[a]	0.75	0.79	0.93[a]
			Three Centers			
σ_{Cu-X-X}	0.37	0.40	0.00	0.40	0.51	0.00
			Unassigned Charge			
ϵ	0.17	0.17	0.11	0.14	0.19	0.10

[a] Contribution is given for directly bonded atoms. For the other Cu–X pairs the contribution is close to zero.

Table IX. Population Analysis Results for Cu_4X_4 Conformers **8–10**

	Cu_4Si_4			Cu_4Sn_4		
	8	**9**	**10**	**8**	**9**	**10**
			Atomic Occupations			
N_X	6.52	6.52	6.63	6.36	6.37	6.49
N_{Cu}	1.10	1.15	1.11	1.24	1.28	1.17
			Atomic Charges			
Q_X	−0.40	−0.34	−0.30	−0.33	−0.27	−0.28
Q_{Cu}	0.50	0.42	0.37	0.41	0.34	0.33
			Two Centers			
σ_{X-X}	1.31	1.79[a] 1.04[b]	1.34	1.18	1.65[a] 0.95[b]	1.21
σ_{Cu-X}	0.48	0.63	0.92	0.53	0.69	0.94
			Three Centers			
σ_{X_3}	0.35	0.30	0.23	0.30	0.27	0.16
σ_{Cu-X_2}	0.21	0.25	0.00	0.21	0.26	0.00
			Four Centers			
σ_{X_4}	0.23	0.18	0.13	0.20	0.16	0.08
σ_{Cu-X_3}	0.14	0.00	0.00	0.12	0.00	0.00
$\sigma_{Cu_2-X_2}$	0.07	0.00	0.00	0.09	0.00	0.00
			Unassigned Charge			
ϵ	0.41	0.32	0.29	0.33	0.25	0.21

[a] For the short X–X distance in the X_4 tetrahedrane. [b] For the capped X_4 tetrahedrane edge.

structures that do not contain tetrahedral X_4 backbones without obtaining a stabilization relative to structure **8** or **9**. These difficulties to distinguish which structure is the most stable one do not occur for the corresponding mixed alkali-metal clusters: for Li_4Si_4 e.g., where structure **8** is clearly favored and the energetic separation is 55 kJ/mol[65] at the SCF level. The small energy difference between structures **8** and **9** finds their expression in the great structural variety of Cu/Si and Cu/Sn phases.[66] Another difference between the M_4X_4 clusters of copper and of the alkali metals is the magnitude of the dimerization energy[67] of the M_2X_2 fragments (Cu_4Si_4, 355 kJ/mol; Cu_4Sn_4, 331 kJ/mol; Li_4Si_4, 270 kJ/mol;[22] Na_4Si_4, 190 kJ/mol[22]). It is to be noted that all structures found to be energetically favored have a tetrahedral X_4 backbone. But contrary to the alkali-metal atoms, the copper atoms are able to occupy both, μ_2- and μ_3-bridging positions, at the X_4 backbone.

(65) SCF energy for **8** is taken from ref 21; calculated geometry and SCF energy for **9**: R_{Si-Si} = 2.30–2.58 Å, R_{Li-Si} = 2.58 Å, E_{SCF} = −15.859 au.
(66) Schubert, K. *Kristallstrukturen zweikomponentiger Phasen*; Springer-Verlag: Berlin, 1964.
(67) The dimerization energy is given as difference between structure **8** and two of its fragments with structure **1**.

Table X. ICSCF Orbital Energies for Cu_2X_2 Conformers **1–3** (hartree)[a]

1		2		3	
		Cu_2Si_2			
$1a_1$	−1.0699	$1a_{1g}$	−1.0705	$1\sigma_g$	−1.0497
$1b_2$	−0.8561	$1b_{2u}$	−0.8538	$1\sigma_u$	−0.8912
$2a_1$	−0.7122	$2a_{1g}$	−0.6730	$2\sigma_g$	−0.7530
$1b_1$	−0.7099	$1b_{3u}$	−0.7494	$1\pi_1$	−0.6509
$3a_1$	−0.6748	$1b_{1u}$	−0.6644		
		Cu_2Sn_2			
$1a_1$	−0.9421	$1a_{1g}$	−0.9403	$1\sigma_g$	−0.9304
$1b_2$	−0.7831	$1b_{2u}$	−0.7834	$1\sigma_u$	−0.8034
$2a_1$	−0.6284	$2a_{1g}$	−0.5875	$2\sigma_g$	−0.6614
$1b_1$	−0.6167	$1b_{3u}$	−0.6569	$1\pi_u$	−0.5620
$3a_1$	−0.5859	$1b_{1u}$	−0.5729		

[a] 1 hartree = 2.626 MJ/mol.

In both cases, Cu_2X_2 and Cu_4X_4, the energetic sequence shows that the bridged structures are favored. These structures have longer X–X and Cu–X bond lengths.

For the more stable structures of the clusters examined in this paper multicenter bonding is a prominent feature. In order to get a quantitative measure, the shared electron numbers were calculated (cf. Tables VIII and IX).[68] Related to the above described increase in the bond lengths for the bridged structures, the two-center-shared electron numbers show a decrease in the bond strength.[69]

The values for CuX_2 three-center bonding in clusters containing copper atoms in μ_2-bridging positions are 0.4–0.5 for Cu_2X_2 (structures **1** and **2**) and 0.25 for Cu_4X_4 (structure **9**). For this contribution, in structure **8** a value of 0.2 is found in both cases, X = Si and Sn (but, it should be considered that the four-center parts are already included). The four-center CuX_3 contribution for a μ_3-bridging position in structure **8** (~0.1) is of the same order of magnitude as the corresponding four-center Cu_2X_2 contribution. Another significant multicenter contribution is found for X_3 and X_4 with values of 0.2 and 0.3, respectively (structures **8** and **9**). In all bridged structures, multicenter contributions are of the same importance as the two-center CuX contributions (three center, structures **1**, **2**, and **9**; four center, structure **8**). For the Cu_2X_2 clusters they are even significantly greater than the two-center parts, if the contribution of the three-center parts is considered. Further indication of multicenter bonding in these clusters is given by the shape of the related LMOs. For all structures except **5** and **7** (σ_{Cu-Cu}: **5**, 0.60; **7**, 0.75), the two-center contribution for the copper–copper interaction is equal to zero. Therefore, it has to be noted that in all energetically favored structures no evidence for copper–copper bonding is found.

Both energetically favored structures **8** and **9** can be described as Zintl compounds having formal X_4^{4-} anions that are isoelectronic to the P_4 molecule.[71] For the Cu_4X_4 clusters with structure **8**, the atomic charges are higher than those of structures **9** and **10** (cf. Table IX). Although lower atomic charges are found in the case of structure **9**, the Zintl picture can be applied in this case as well. This is due to the similar MO structure. The difference mainly is that in the case of structure **9** a bonding interaction is found along the stretched tetrahedrane edges, indicated by the two-center-shared electron number (see Table IX).

The relation between the relatively high thermodynamic stability of the bridged structures and the fact that multicenter bonding becomes a dominant feature need, however, some more investigation. The energies of the ICSCF orbitals might help us to get more information about the various energy contributions to the

Table XI. ICSCF Orbital Energies for Cu_4X_4 Conformers **8–10** (hartree)[a]

8		9		10	
		Cu_4Si_4			
$1a_1$	−1.1676	$1a_1$	−1.1454	$1a_1$	−1.1616
$1t_2$	−0.9375	$1b_2$	−0.9599	$1t_2$	−0.9197
		1e	−0.9224		
$2a_1$	−0.7114	$2a_1$	−0.7316	$2a_1$	−0.7838
$2t_2$	−0.6932	$2b_2$	−0.6838	$2t_2$	−0.6980
		2e	−0.6779		
1e	−0.6546	$3a_1$	−0.6745	1e	−0.6217
		$1b_1$	−0.6864		
		Cu_4Sn_4			
$1a_1$	−1.0097	$1a_1$	−0.9941	$1a_1$	−1.0060
$1t_2$	−0.8404	$1b_2$	−0.8607	$1t_2$	−0.8275
		1e	−0.8288		
$2t_2$	−0.6213	$2b_2$	−0.5933	$2a_1$	−0.6880
		2e	−0.6032	$2t_2$	−0.6114
$2a_1$	−0.6061	$2a_1$	−0.6267		
1e	−0.5737	$3a_1$	−0.5899	1e	−0.5428
		$1b_1$	−0.6192		

[a] 1 hartree = 2.626 MJ/mol.

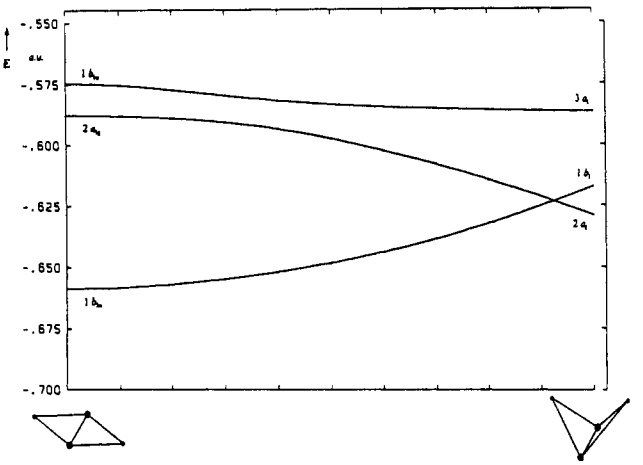

Figure 3. ICSCF orbital energy correlation diagram of structures **1** and **2** for Cu_2Sn_2. The energies are given as a function of the angle between the $CuSn_2$ planes.

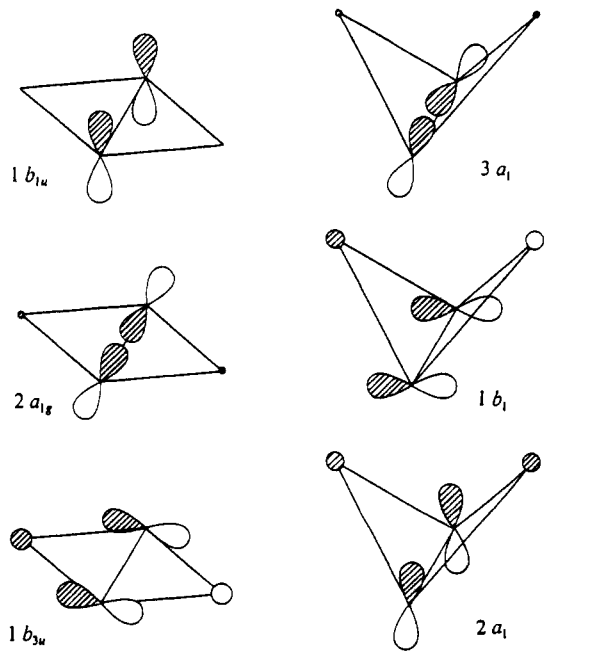

Figure 4. Schematic shapes of the three highest ICSCF orbitals of structures **1** and **2** for Cu_2Sn_2 clusters.

(68) The relatively high unassigned charges are due to the use of unmodified atomic orbitals.
(69) A correlation is found between the bond length and the two center-shared electron numbers σ', if the latter are modified by subtracting the contributions of higher order, according to Pauling's equation: $d = d_1 - n \log \sigma'$ (e.g.: Si–Si, d_1 = 2.34 Å, n = 0.64 Å; Sn–Sn; d_1 = 2.83 Å, n = 0.78 Å; for comparison the covalent radii are 1.17 Å for Si and 1.40 Å for Sn[70]).
(70) Pauling, L. *The Nature of the Chemical Bond*, 3rd ed.; Cornell University Press: Ithaca, NY, 1960.
(71) von Schnering, H. G. *Nova Acta Leopold.* **1985**, *59*, 165.

Table XII. Population Analysis Results for the Calculated LMOs of Structure **1** for Cu_2X_2 Clusters

type of LMO	loc	N_μ			$\sigma_{\mu\nu}$			$\sigma_{\lambda\mu\nu}$		
					Cu_2Si_2					
lone pair[a]	0.95	s(Si)	1.17	0.62						
		p(Si)	0.72	0.38						
Si–Si σ bond[b]	0.93	s(Si)	0.49		s(Si)–s(Si)	0.24	0.16			
		p(Si)	1.04		p(Si)–p(Si)	0.50	0.33			
					s(Si)–p(Si)	0.37	0.25			
μ_2 bridge[b] (Cu–Si_2 bond)	0.99	s(Si)	0.16		s(Si)–s(Si)	0.08		s(Si)–s(Si)–s(Cu)	0.08	0.12
		p(Si)	1.15		p(Si)–p(Si)	0.56		p(Si)–p(Si)–s(Cu)	0.38	0.60
		s(Cu)	1.09		s(Si)–p(Si)	0.09		s(Si)–p(Si)–s(Cu)	0.09	0.14
					s(Si)–s(Cu)	0.16				
					p(Si)–s(Cu)	0.62				
					Cu_2Sn_2					
lone pair[a]	0.95	s(Sn)	1.31	0.69						
		p(Sn)	0.59	0.31						
Sn–Sn σ bond[b]	0.93	s(Sn)	0.43		s(Sn)–s(Sn)	0.17	0.12			
		p(Sn)	1.08		p(Sn)–p(Sn)	0.54	0.39			
					s(Sn)–p(Sn)	0.34	0.25			
μ_2 bridge[b] (Cu–Sn_2 bond)	0.99	s(Sn)	0.12		s(Sn)–s(Sn)	0.05		s(Sn)–s(Sn)–s(Cu)	0.05	0.09
		p(Sn)	1.08		p(Sn)–p(Sn)	0.49		p(Sn)–p(Sn)–s(Cu)	0.38	0.67
		s(Cu)	1.29		s(Sn)–p(Sn)	0.07		s(Sn)–p(Sn)–s(Cu)	0.07	0.12
					s(Sn)–s(Cu)	0.12				
					p(Sn)–s(Cu)	0.69				

[a] For the lone pairs the fraction of s and p AO character is given. [b] For the chemical bonds the fraction of the shared electron numbers between AOs with respect to the shared electron number of the related atoms is given.

stability of the clusters examined here. We therefore calculated ICSCF orbital energies, which sum to the total energy of the cluster (cf. Tables X and XI).

The stabilization of π orbitals and destablization of the σ orbitals for the Cu_2X_2 clusters from **3** to **2** and from **3** to **1** is evident from simple symmetry arguments. In both cases, the destabilization of the highest σ orbital is exceeded by the stabilization of the π orbitals. For structures **1** and **2** significant changes in orbital energies were only observed for the three highest occupied orbitals (cf. Table X).

Figure 3 shows the correlation diagram of the ICSCF orbital energies and the angle between the two Cu–Sn_2 planes for the structures **1** and **2** of Cu_2Sn_2. The corresponding orbital shapes are given in Figure 4. For these two structures, the most pronounced effects are observed on the two π-bonding-type orbitals (**2**, $1b_{1u}$, $1b_{3u}$; **1**, $2a_1$, $1b_1$). From **2** to **1**, the stabilization of the highest π-bonding-type orbital exceeds the destabilization of the lower one. The orbital energy of the σ-bonding-type orbital in both structures (**2**, $2a_{1g}$; **1**, $3a_1$) is nearly left unchanged. Obviously, the fact that the change in the orbital energy of the highest occupied molecular orbital (HOMO) reproduces quite well the energy differences between the conformers (cf. also ref 22) would not appear without the avoided crossing between the two highest orbitals of structure **2** ($1b_{1u}$ and $2a_{1g}$; cf. Figure 3). This property of the HOMO (reproduction of the total energy difference) in the Cu_2X_2 clusters holds also for the Cu_4X_4 clusters with structures **8** and **10** but not for structure **9**. For the Cu_4X_4 clusters the competition between the μ_2- and μ_3-bridging position of the copper atoms manifests itself in the nearly unchanged ICSCF energies of the corresponding orbitals (e.g.: **8**, $2t_2$, $2a_1$; **9**, $2a_1$, $2b_2$, $2e$).

To summarize the results given above, it has to be noted that the high multicenter bonding contributions for bridged structures like **1** and **2** (Cu_2X_2) and **8** and **9** (Cu_4X_4) seem to be characteristic of the heavier elements of the group 14 like silicon and tin (cf. also ref 22). For carbon, two-center bonds are favored, as is well-known in the case of C_2H_2. Only in the case of lithium-containing carbon clusters were bridged structures found (cf. ref 20), but their most stable structures and bonding situation are clearly different from those observed for the heavier elements of the group 14.

The type of bonding in mixed Cu_2X_2 and Cu_4X_4 clusters is closely related to the so-called "inert pair effect",[72] which means that for heavier main-group elements not all the valence electrons are accessible to chemical bonding. In order to investigate this behavior, related with chemical bonds and lone pairs, the LMOs of the clusters were calculated. Each LMO was analyzed by the formerly described method of population analysis to investigate the s and p AO contribution to the chemical bonds and lone pairs (see Tables XII and XIII). Therefore, the occupation of the AOs and the shared electron numbers for pairs and triples of AOs related to the corresponding LMO were calculated. Also, the fraction of localization and the fraction of the shared electron numbers for pairs and triples of AOs with respect to the total two- and three-center-shared electron number of the corresponding atoms are listed in Tables XII and XIII. The fraction of localization is defined as

$$\text{localization} = \frac{N_{\text{LMO}}}{N_{\text{tot}}} \qquad (3)$$

where N_{LMO} and N_{tot} denote the occupation of the AOs mainly involved in the LMO and the occupation of all AOs of the minimal basis set used in the projection, respectively. The shared electron number for pairs and triples of AOs are defined according to that of pairs and triples of atoms.[61,62] N_μ(A) denotes the occupation

Table XIII. Population Analysis Results for the Calculated LMOs of Structure **3** for Cu_2X_2 Clusters[a]

type of LMO	loc	N_μ		$\sigma_{\mu\nu}$		
			Cu_2Si_2			
Si–Si σ bond	0.99	s(Si)	0.84	s(Si)–s(Si)	0.46	0.22
		p(Si)	0.95	p(Si)–p(Si)	0.41	0.20
				s(Si)–p(Si)	0.60	0.29
Cu–Si σ bond	0.99	s(Si)	1.06	s(Si)–s(Cu)	0.60	0.52
		p(Si)	0.84	p(Si)–s(Cu)	0.54	0.48
		s(Cu)	1.01			
Si–Si π bond	1.00	p(Si)	1.37	p(Si)–p(Si)	0.75	
			Cu_2Sn_2			
Sn–Sn σ bond	0.99	s(Sn)	0.80	s(Sn)–s(Sn)	0.38	0.19
		p(Sn)	0.96	p(Sn)–p(Sn)	0.47	0.24
				s(Sn)–p(Sn)	0.57	0.29
Cu–Sn σ bond	0.99	s(Sn)	1.10	s(Sn)–s(Cu)	0.60	0.51
		p(Sn)	0.80	p(Sn)–s(Cu)	0.58	0.49
		s(Cu)	1.05			
Sn–Sn π bond	1.00	p(Sn)	1.34	p(Sn)–p(Sn)	0.69	

[a] For the LMOs the fraction of the shared electron numbers between AOs with respect to the shared electron number of the related atoms is given.

(72) For example, see: Murrell, J. N.; Kettle, S. F. A.; Tedder, J. M. *Valence Theory*; Wiley: London, 1965.

Table XIV. Relative Energy for Cu_2X_2 Conformers (1–3) Relative to Structure 1 (at SCF Level) with s Orbitals Kept Frozen and Free (mhartree)[a]

	electronic state	s free	s frozen
		Cu_2Si_2	
1	$^1A_1$	0.0	0.0 (54.2)[b]
2	$^1A_{1g}$	23.6	31.6
3	$^1\Sigma_g^+$	54.2	150.7
		Cu_2Sn_2	
1	$^1A_1$	0.0	0.0 (34.8)[b]
2	$^1A_{1g}$	30.6	31.3
3	$^1\Sigma_g^+$	73.8	159.8

[a] 1 mhartree = 2.626 kJ/mol. [b] Energy difference relative to structure 1 without frozen s orbitals.

of the μ AO on atom A, and $\sigma_{\mu\nu}(AB)$, the shared electron number between the two AOs μ and ν on the atoms A and B, e.g.

$$\sigma_{\mu\nu}(AB) = N_\mu(A) + N_\nu(B) - N_{\mu\nu}(AB) \quad (4)$$

The conformations 1–3 of the Cu_2X_2 clusters are suitable model structures to investigate the inert pair effect and the different contributions of s and p symmetry AOs to chemical bonding. Especially the s AO contribution is basically different, due to the symmetry constraints, for the bridged structures 1 and 2 and the linear one 3. For structure 3 the s AO contributions of the X atoms are necessary to build up all σ bonds (X–X and Cu–X). Therefore, only in bridged structures an "inert pair" occurs on the X atoms (e.g. structure 1 in Table XII). The s character of these inert pairs increases as X changes from silicon to tin. Although the s character is dominant for the inert pairs, they have p contributions due to the so-called Pauli repulsion.[73] In both structures 1 and 3 for the bonding LMOs a p–p contribution is found, but they are quantitatively different (see Tables XII and XIII). The main difference is found for the copper bonding LMOs (μ_2-bridging Cu–X_2 bonds for structure 1 and Cu–X σ bonds for structure 3). In structure 1 the three-center Cu–X_2 bonds have a high p(X) AO contribution given by the fraction of the p(X)–p(X)–s(Cu) shared electron number with respect to the total three-center-shared electron number (Table XII). For structure 3 the p(X) AO contribution in the copper bonding LMO is lower than in structure 1.

The valence configuration for the X atoms in structure 1 of the Cu_2X_2 clusters roughly corresponds to s^2p^2, on the basis of calculated LMOs[74] (X = Si, $s^{1.88}p^{2.50}$; X = Sn, $s^{1.92}p^{2.31}$). This gives further evidence for an "inert s shell" in the case of the bridged structure 1 of the Cu_2X_2 clusters. For the linear structure 3 the valence configuration is clearly different from s^2p^2 (X = Si, $s^{1.38}p^{3.32}$; X = Sn, $s^{1.51}p^{3.10}$). Because of the energetic stability of structure 1 relative to structure 3, the s^2p^2 valence configuration seems to be favored.

The inert pair effect indicated by the occurrence of lone pairs is connected with a high multicenter bonding contribution for the corresponding structures. A further indication for an inert pair is given by the nearly unchanged energies of the two low-lying ICSCF orbitals in the structures 1 and 2 for Cu_2X_2 (see Table X).

As a consequence of the inert pairs, it should be possible to treat the heavier elements of the group 14 as two-valence-electron atoms. To investigate this expectation, we performed molecular calculations where the s orbitals of the X atoms are kept frozen[75] and the structures were reoptimized. By the reoptimization of the structures only the X–X bond length is slightly increased (0.1–0.2 Å) due to increase of the so-called Pauli repulsion by freezing the s orbitals of the X atoms. The relative energy differences for full variational and frozen-core calculations are given in Table XIV; both were done at the SCF level. In the case of Cu_2Sn_2 the energy differences between structures 1 and 2 are practically the same whether the orbitals are frozen or not, while this is not the case for 3, in accordance with the results of the population analysis. These calculations also show that the inert pair effect increases from silicon to tin.

Let us turn now to a brief discussion of the underlying reasons for the inert pair effect. The existence of an inert pair of electrons in the heavier elements of the main groups was postulated by Sidgwick[76] to explain the phenomenon that they form compounds where two of the valence electrons are not involved in bonding and remain formally unoxidized.

A formerly often used argument is the reluctance of "s" electrons to participate in bond formation, because of the completion of the "s" shell.[77] If this explanation were correct, the ionization potential of the s electrons should increase within a family of elements, but this is obviously not the case (cf. ref 73).

The $6s^2$ inert pair is sometimes related to (see ref 48 and references therein) the relativistic increase of the s–p energy difference from tin to lead. However, compounds with lower valence are known also for lower periods (such as $GeCl_2$ and $SnCl_2$[78]). For these elements relativity certainly cannot be advocated to explain the $4s^2$ and $5s^2$ inert pairs. Generally, it has to be noted that more than the variation of the s–p energy difference within a family is required to explain the inert pair effect. This is obviously seen for the elements of the group 14 (Δ(s–p): C, 8.32 eV; Si, 7.25 eV; Ge, 8.11 eV; Sn, 6.88 eV; Pb, 7.93 eV).[79,80] Indeed, the $6s^2$ inert pair for lead is related to a high s–p energy difference. The s–p energy difference for silicon and tin is quite the same, however, while the tendency to form compounds of lower valence is clearly different.

The explanation of the inert pair effect given by Drago in 1958 by thermodynamic arguments[81] is a currently accepted one (see for example ref 78). Drago has shown with thermodynamic data that for the chlorides of group 13 and of group 14 elements weaker covalent bonds will be formed with increasing nuclear charge. Given the weaker covalent bonds for the heavier elements, there is not enough energy to compensate for the promotion needed in the higher valence case. Bonding can occur, of course, by using mainly the p orbitals. Such a behavior is found for the Cu_2X_2 clusters as shown above.

Why are bonds weaker with increasing nuclear charge? The answer is given most easily by analyzing the shape of the pseudopotentials.[82,83] The magnitude of the attractive part of the pseudopotentials, $-Q/r$, is the same for all elements within a group of the periodic table, where Q stands for the charge of the core. On the other hand, a larger core size is found for the heavier elements, leading to a reduction of the depth of the attractive well and to a minimum at larger distance (for the pseudopotentials used in this work, see ref 84; cf. also ref 85).

Summarizing, it must be noted that the explanation for the inert pair effect by Drago[81] is still valid and can be based on quantum mechanical arguments.

Conclusion

In the present pseudopotential study on mixed Cu_2X_2 and Cu_4X_4 clusters (X = Si, Sn) it is shown that the copper atoms prefer bridged positions in all cases.

The dimerization energy of the Cu_2X_2 clusters is found to be considerably greater than that for the corresponding alkali-metal

(73) Kutzelnigg, W. *Angew. Chem.* **1984**, *96*, 262.
(74) The occupation numbers were taken from a Mulliken population analysis of the calculated LMOs.
(75) The coefficients were taken from atomic calculations for the ground states.
(76) Sidgwick, N. V. *Annu. Rep.* **1933**, *20*, 120.
(77) Grimm, H. G.; Sommerfeld, A. *Z. Phys.* **1926**, *36*, 36.
(78) Greenwood, N. N.; Earnshaw, A. *Chemistry of the Elements*; Pergamon: Oxford, England, 1984.
(79) The s–p gap is given as difference between the valence shell ns and $np_{1/2}$ orbital energies.
(80) Desclaux, J. P. *At. Data Nucl. Data Tables* **1973**, *12*, 311.
(81) Drago, R. S. *J. Phys. Chem.* **1958**, *62*, 353.
(82) Durand, P.; Barthelat, J. C. *Theor. Chim. Acta* **1975**, *38*, 283.
(83) For graphical representations the pseudopotential V (see eq 2) plus the centrifugal term is employed here: $U_l(r) = V_l(r) + l(l+1)/2r^2$.
(84) Kohout, M. Technical Report (20.10.1987); Institut für Theoretische Chemie: University of Stuttgart, West Germany, 1987.
(85) Zunger, A. *Phys. Rev. B* **1980**, *22*, 5839.

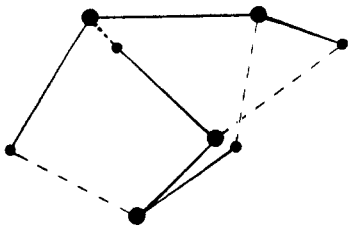

Figure 5. Two twisted trans-bent Cu_2X_2 units building up the μ_2-bridged tetrahedral structure **9**.

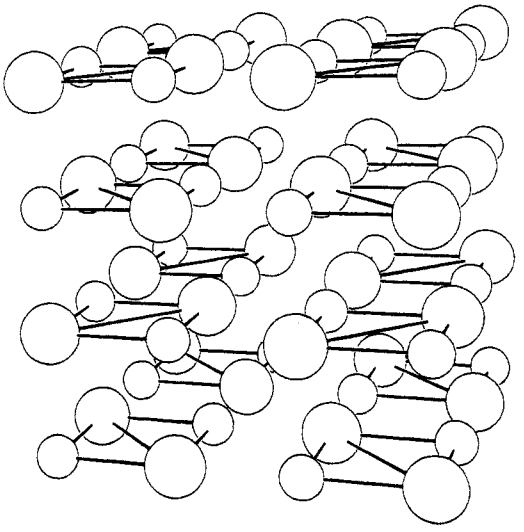

Figure 6. Planar μ_2-bridged M_2X_2 clusters building up the NaCl-type crystal structure.

clusters. The bent μ_2-Cu_2X_2 cluster can be regarded as a prestructure of the μ_3-Cu_4X_4 heterocubane.

Our calculations indicate that for Cu_4X_4 clusters the μ_3-Cu_4X_4 heterocubane structure is favored. Moreover, a novel structure with four tetrahedral edges capped by copper atoms in μ_2-bridging positions was found. The energy separation between the heterocubane and this novel structure is significantly smaller than that for the related alkali-metal compounds. In all cases the X atom backbone (X_2 and X_4) determines the structure and no evidence for copper–copper bonding is found. But the copper atoms surely have an influence on the chosen geometry, which is indicated by the low energetic separation between the μ_3-bridged heterocubane and the novel μ_2-bridged X_4 tetrahedra.

An interesting feature in the case of the novel μ_2-bridged tetrahedral structure is the fact that this structure can be also described as a nontetrahedral structure, which is formally composed of two twisted trans-bent Cu_2X_2 units (see Figure 5). Therefore, this structure can be regarded as an intermediate structure on the route from the heterocubane to two separate monomeric Cu_2X_2 units, where a twisted cyclobutadiene analogue might be a transition state.

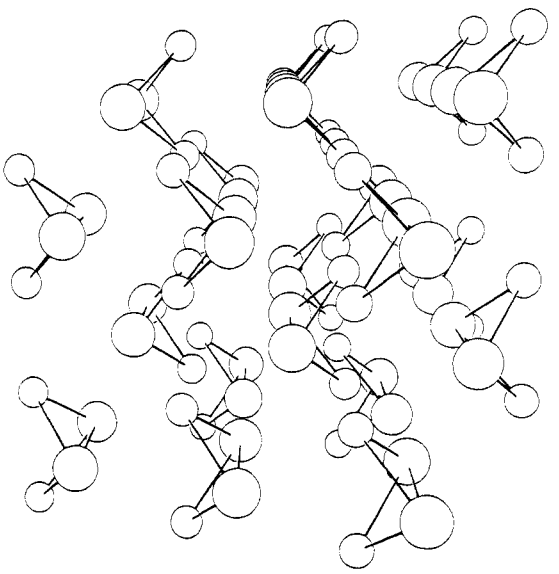

Figure 7. M_2X_2 clusters with butterfly geometry building up the NiAs-type crystal structure.

In relation with solid-state structures for AB compounds the M_2X_2 clusters can be regarded as prestructures, e.g. the planar and bent μ_2-M_2X_2 clusters for the NaCl-type and NiAs-type structures, respectively (see Figures 6 and 7).

For compounds with a NiAs-type crystal structure it is a well-known fact that electrostatic interaction is no longer the dominant feature in contrast to the case for NaCl-type structures.[86] For CuSn the NiAs-type crystal structure[66] is found. This is in good agreement with the fact that the most stable structure for Cu_2Sn_2 clusters is the bent double-bridged one, with a clear energetic separation relative to the planar μ_2-bridged structure. Curiously, the angle between the two bent $CuSn_2$ planes for the Cu_2Sn_2 cluster (81.5°) is nearly the same as in the corresponding butterfly prestructure of the CuSn crystal structure (~85°).[66]

Finally, it has been shown that the "inert pair effect" is well described by trends of the pseudopotentials within a family of elements. Both the increasing distance from the nucleus and the reduced depth of the pseudopotentials support the thermodynamic arguments of Drago.

Acknowledgment. We wish to thank Prof. K. A. Gingerich for the stimulating discussions that were at the origin of the present work. Thanks are due to M. Dolg, Dr. G. Igel-Mann, and M. Kohout for valuable discussions. The financial support of the Deutsche Forschungsgemeinschaft is gratefully acknowledged.

Registry No. Cu_2Si_2, 124821-98-3; Cu_4Si_4, 124821-99-4; Cu·Sn, 12054-11-4.

(86) Wells, A. F. *Structural Inorganic Chemistry*, 5th ed.; Clarendon Press: Oxford, England, 1984.